

# Study of Weak Electric Current Emissions on Cement Mortar under Uniaxial Compressional Mechanical Stress up to the Vicinity of Fracture

Antonios Kyriazopoulos\* - Ilias Stavrakas - Cimon Anastasiadis - Dimos Triantis  
Laboratory of Electric Properties of Materials, Department of Electronics,  
Technological Educational Institution of Athens, Greece

*An experimental technique that deals with the detection of weak electric signals emitted during the application of temporal uniaxial stress on solid materials has been applied on cement mortar samples. These electric signals are met in the literature as Pressure Stimulated Currents (PSC). Two different stress techniques were applied: uniaxial compressional stress at a) a low and b) at a high rate. Both qualitative and quantitative characteristics of the PSC are correlated with the mechanical state of the samples with respect to crack creation and propagation in the bulk of the material and consequently with the stages of composite damage.*

©2011 Journal of Mechanical Engineering. All rights reserved.

**Keywords:** cement mortar, electric current emissions, PSC, uniaxial stress, microcracks

## 0 INTRODUCTION

It has been experimentally verified that mechanical stress application on geo-material samples is accompanied by the production of weak electric variations. Several laboratory experiments have been conducted to study the behaviour of geo-material samples under stress and have showed electromagnetic activity as well as electric current emissions. More precisely, experiments have been conducted on rock specimens suggesting that electric signals are produced by the piezoelectric effect due to presence of quartz [1] and [2], electrokinetic effect due to water movement [3] and [4], point defects [5] and [6], emission of electrons [7] and [8], moving charged dislocations (MCD) [9] to [11].

Laboratory experiments to detect and record weak transient current produced when brittle materials like marble and amphibolite are subjected to a temporal stress variation leading to a catastrophic process up to fracture have recently been realised [11] to [16]. The above mentioned electric currents are met under the term Pressure Stimulated Currents (PSC) and the corresponding experimental technique is known as Pressure Stimulated Currents technique.

In the present work for the very first time the PSC technique is applied on cement

mortar samples and the results after systematic recordings are presented here. In this work, various experimental techniques showing up PSC were applied on cement mortar samples and PSC measurements were systematically recorded.

Electric emissions in cement mortar under low compressional loading (less than 30% of compressional strength) have also been observed by other researchers [17] and were attributed to various mechanisms including crack opening. Additionally, electric current emissions have been recently reported on hardened cement paste and were attributed to the Piezoelectric effect [18].

A satisfactory interpretation of electric signal emission during the deformation of brittle materials after stress application is attributed to mechanisms of crack generation and propagation as well as to the moving charged dislocations by a number of researchers [9], [19] and [20]. According to the MCD model in an ionic or composite amorphous structure there will be an excess or absence of a line of ions along the dislocation line, with the consequence that the dislocation be charged. In thermal equilibrium, dislocation lines are surrounded by the Debye-Hueckel charge cloud and will be electrically neutral [21]. In dynamic processes when dislocations move faster than the Debye-Hueckel cloud can follow, neutrality can no longer be

\*Corr. Author's Address: Laboratory of Electric Properties of Materials, Department of Electronics, Technological Educational Institution of Athens, Athens, 12210, Greece, akryiazo@teiath.gr

maintained. It has been proved that when a brittle material is uniaxially compressed with a time varying stress  $\sigma$ , the Pressure Stimulated Current is proportional to the strain rate [11]:

$$I \propto \frac{d\varepsilon}{dt} \propto \frac{1}{E} \cdot \frac{d\sigma}{dt}, \quad (1)$$

where  $d\varepsilon/dt$  is the compressional strain rate,  $d\sigma/dt$  is the stress rate and  $E$  is the modulus of elasticity.  $E$  is constant in the linear-elastic behaviour range while it varies in the non-linear deformation range and in the localized failure crack zone that follows, as a result of microcrack formation. As can be seen, Eq. (1) which comes from the MCD model is a tool giving qualitative rather than quantitative information.

### 1 DESCRIPTION OF THE EXPERIMENTAL TECHNIQUES

Two groups of PSC recording experiments are presented and they refer to the case when the samples suffer a uniaxial compressional stress.

In the first group, the uniaxially applied stress  $\sigma$  is increasing linearly at a slow rate described by:

$$\sigma = a \cdot t, \quad (2)$$

where  $a$  is the stress rate, the values of which do not usually exceed 500 kPa/s and the ordinary values are around 100 kPa/s. At  $t = t_f = \sigma_{max} / a$ , where  $\sigma_{max}$  is the ultimate compressional stress, the sample fails. This experimental technique henceforth will be referred to as Low Stress Rate Technique (LSRT).

In the second group, while the sample is in a state of constant uniaxial stress  $\sigma_k$ , an abrupt stepwise stress increase of short duration  $\Delta t$  is applied so that the uniaxial stress increases by  $\Delta\sigma = \sigma_{k+1} - \sigma_k$ , where  $\sigma_{k+1}$  is the new state after the application of the stress increment (see Fig. 1). It must be noted that the new stress state  $\sigma_{k+1}$  remains constant until a following stress increment is applied. The aforementioned temporal variation of stress  $\sigma$ , as recorded during this experimental procedure can be described in a good approximation by Eq. 3.

$$\sigma(t) = \begin{cases} \sigma_k = \text{constant} & \text{for } t < t_k \\ \sigma_k + b(t - t_k) & \text{for } t_k < t < t_{k+1} \\ \sigma_{k+1} = \text{constant} & \text{for } t > t_{k+1} \end{cases}, \quad (3)$$

This stepwise stress technique hereafter called Step Stress Technique (SST) is suitable to expose PSC in both the linear and non-linear ranges of the material deformation. Typical values of stress rate  $\sigma$  vary between 1.5 and 5 MPa/s and are always greater than those of the LSRT technique.

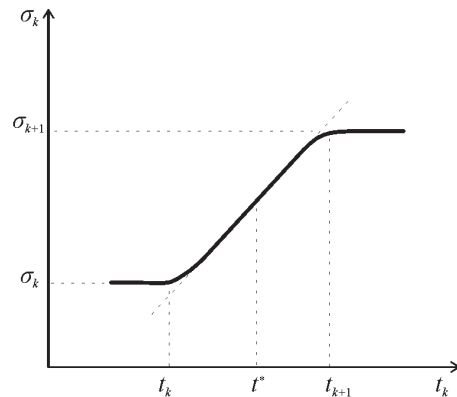


Fig. 1. Schematic representation of uniaxial stress  $\sigma$  variation with respect to time as it was recorded experimentally using the Step Stress Technique

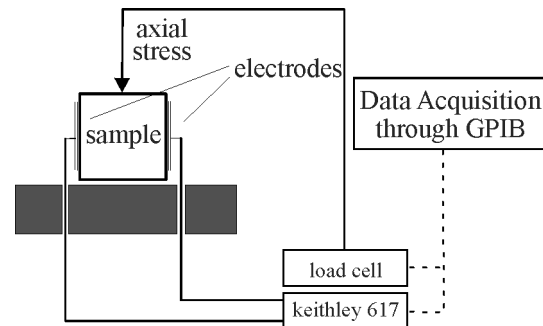


Fig. 2. Schematic representation of the SST and LSRT experimental techniques

Fig. 2 shows the schematic representation of the SST and LSRT experimental techniques. A pair of electrodes was attached to the sample in a direction perpendicular to the axis of the applied stress and the PSC measurements were achieved using a sensitive programmable electrometer (Keithley 6514) and all data were stored in a computer hard disk through a GPIB interface. The stressing system comprised an uniaxial hydraulic load machine (Enerpac-RC106) that applied compressional stress to the sample.

The experiment was conducted in a Faraday shield to prevent electric noise. Between each sample and the stressing system thin Teflon plates were placed in the direction of stress, in order to provide electrical insulation. The electrodes were attached to the cement mortar sample, using conductive paste.

## 2 SAMPLES

Cement mortar samples were used, composed of Portland type cement OPC (Ordinary Portland Cement), sand and water at a ratio 1:3:0.5 respectively. The samples were utilized 3 months after their preparation in order to age properly and achieve an approximate 95% of their maximum strength. The maximum diameter of the sand grains of the composition was 2 mm. Its density was 2.2 gr/cm<sup>3</sup> and its porosity was approximately 8%.

Table 1 incorporates the characteristics of the samples including their geometric shapes, the fracture limits and the applied stress or load rates for each experimental technique.

Fig. 3 shows a representative relative compressional stress ( $\hat{\sigma}$ ) - strain ( $\epsilon$ ) curve of the used samples. The relative compressional stress value is given as  $\hat{\sigma} = \sigma / \sigma_{max}$ , where  $\sigma_{max}$  is the ultimate compressional stress. It is evident that it can be characterized by a linear material behavior at least up to stresses of 70% ( $\hat{\sigma} = 0.7$ ) approximately of the ultimate compressional stress. In this range the material is characterized by a linear-elastic behavior and an elasticity modulus  $E$ . The stress  $\sigma$  on the material is related to the deformation  $\epsilon$  (i.e. strain) according to the following linear law:

$$\sigma = E_0 \cdot \epsilon, \quad (4)$$

where  $E_0$  is the elasticity modulus of the undamaged material and according to the experimental data presented in the stress - strain curve  $E_0 = 13$  GPa approximately. When the

relative compressional stress acquires values greater than 0.7 approximately, the material is driven to a range of non-linear deformation and eventually into the localized failure zone.

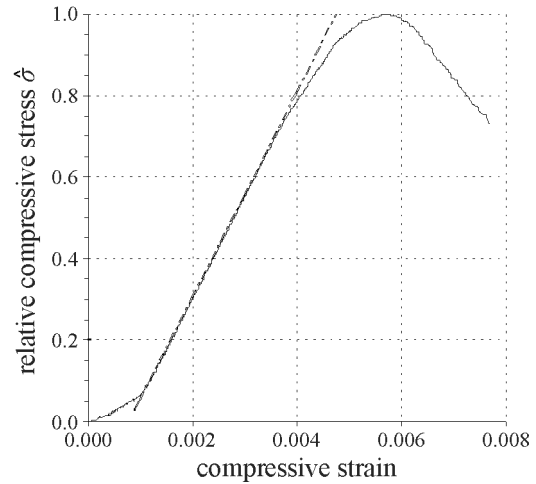


Fig. 3. Stress-strain diagram of the used cement mortar samples; the stress axis corresponds to the relative compressive stress

## 3 EXPERIMENTAL RESULTS AND DISCUSSION

Representative PSC recordings from a set of experiments using both of the referred techniques (LSRT and SST) were conducted. The PSC recordings from the respective experiments are characterized by a systematic repeatability if all experimental requirements are carefully satisfied.

In the first type of experiments (LSRT), the samples were loaded at a constant positive uniaxial stress rate 0.18 MPa/s. Fig. 4 depicts the recordings of the PSC emitted from cement mortar along with the relative compressional stress. As long as the sample is stressed uniaxially at low stress values corresponding to relative

Table 1. Characteristics of the samples, and parameters of the applied experimental techniques

Sample Code	Dimensions [mm]	Fracture limit [MPa]	Experimental technique	Stress rate [MPa/s]
CM01	50 x 50 x 70	59	LSRT	0.18 ± 0.01
CM02	50 x 50 x 70	52	SST	5.0 ± 0.1

compressional stress values lower than 0.65 approximately, the PSC values are very small. According to what Eq. (1) indicates and given that in the LSRT technique ( $d\sigma / dt = \text{const.}$ ) no PSC appearance should be expected in a range of relative compressional stress less than 0.65. The fact that a very weak but distinguishable PSC is recorded, must be related with the activation of some microcracks which might start from the interfaces between grains and cement especially in regions of the material near the compressed surfaces of the sample.

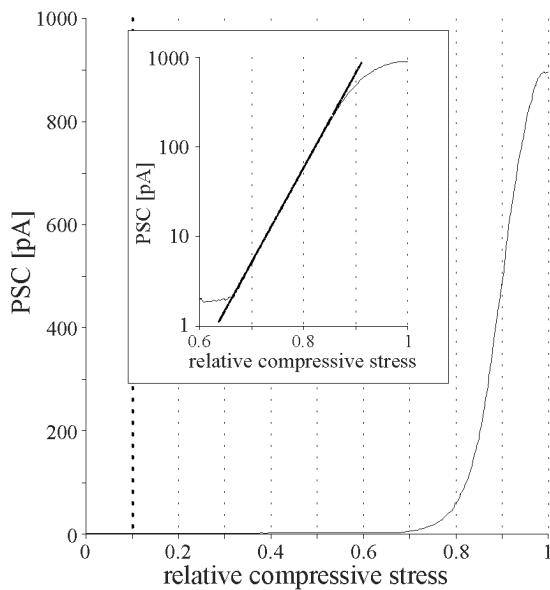


Fig. 4. The behaviour of PSC with respect to linearly increasing stress (Low Stress Rate Technique); in the inset graph the PSC is shown on a logarithmic axis for  $\hat{\sigma} > 0.6$

When the relative compressional stress upon the sample becomes greater than 0.65 approximately, then, a very intense exponential increase of the PSC values is observed which is directly related with the fact that the material has been driven into the non linear deformation range (see Fig. 3). In this range the elasticity modulus gradually decreases and a PSC emission is also expected by Eq. (1). The PSC values increase rapidly and continuously up to the failure limit. In this range microcracks occur leading to the appearance of fresh surfaces due to bond breaking and lattice destruction. The appearance

of localized charges is expected as a consequence of this. On the other hand, it has been observed on cement mortar samples that no measurable compressional stress – induced cracks have been formed before stress approaching 70% of the ultimate stress had been reached [22].

As can be seen in Fig. 4 the recorded PSC is a weak systematically increasing transient current. Although the creation and propagation of a microcrack is a random phenomenon in the catastrophic process, there is nevertheless, always a first microcrack which develops to a main – mother – crack defining a dominant orientation. Consequently, there must be a dominant current component whose orientation is related with the mother crack orientation. Evidently, the measured PSC corresponds to one or more of the current components which are definitely different from zero as has been proved experimentally.

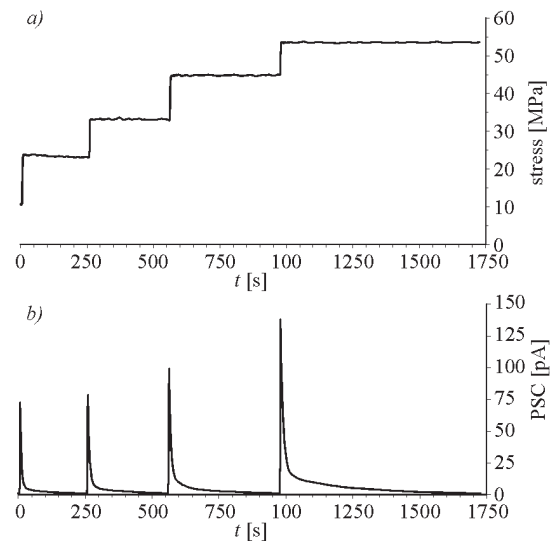


Fig. 5. a) Presentation of the stepwise stress steps, b) the corresponding PSC recordings with respect to time

If the PSC values are correlated with the relative compressional stress values  $\hat{\sigma}$  in the range (zone nonlinear deformation) ( $0.7 < \hat{\sigma} < 0.85$ ) then, as can be seen in the inset diagram of Fig. 4, they are described by an exponential law of the form:

$$I = I_0 \cdot \exp(\alpha \cdot \hat{\sigma}), \quad (5)$$

where  $I_0$  is a current constant and the characteristic exponent  $\alpha$  describing the magnitude of the PSC increase in the referred range, (after fitting) has a value  $\alpha \approx 24$ . The deviations of PSC values from the exponential law are evident when the relative compressional stress becomes greater than the value ( $\hat{\sigma} \approx 0.85$ ), a value corresponding to a transition zone signaling the onset of unstable crack growth and the material enters a localized failure crack zone. In this range the PSC values keep on increasing intensely and as the ultimate strength point is reached, the PSC gets to a maximum.

During the second type of experiment (SST), four sequential abrupt stress increases at a constant rate ( $b = 5 \text{ MPa/s}$  approximately) were performed (see Fig. 5a). The temporal variation of the PSC during the above procedure is depicted in the diagram of Fig. 5b. On application of each abrupt stepwise uniaxial compressional stress, an equally abrupt current spike appears, having a peak at a value  $PSC_{\text{peak}}$ , as soon as the stress gets to the final state  $\sigma_k + 1$ . It should be noted that the appearance of the PSC is due to the abrupt application of stress even at low stress levels. The abrupt stress increase during the stepwise stress procedure produces an inhomogeneous stress field within the non-homogeneous structure of the material under compression. When the local stress exceeds local strength, then, a microcrack occurs. During a microcrack opening two fresh surfaces are produced in the bulk of the material since the bonds are broken and the lattice is destroyed. These new surfaces are responsible for the charge separation phenomenon. Instantaneous charges are produced due to the destruction of the lattice and weak electric currents flow in order to get the distorted equilibrium state to a new stable equilibrium state. Thus, the  $PSC_{\text{peak}}$  can be interpreted. During microcrack creation and the consequent charge appearance, a time-varying microcurrent appears around the microcrack. The recorded PSC is the superposition of such microcurrents. Its magnitude gets to a maximum when the local concentration of microcracks gets also to a maximum.

Particularly, when two or more cracks meet a hard aggregate particle like sand grain, they merge leading to the generation and propagation of a mother crack so that instead of a single

crack advancing, a whole family of cracks could gradually be formed, and this requires larger forces and uses more energy.

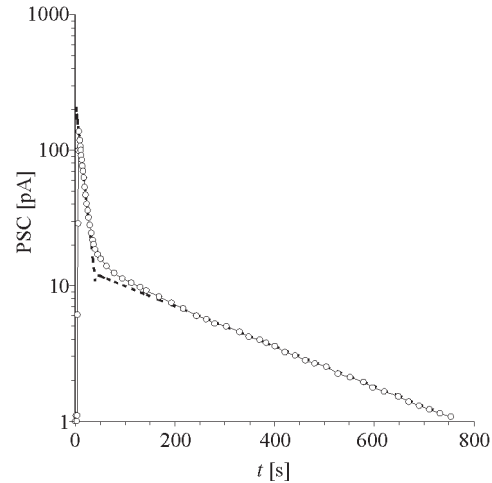


Fig. 6. The two relaxation mechanisms of the fourth step are characterized by two different slopes

Accordingly, after the appearance of  $PSC_{\text{peak}}$ , relaxations of a complex exponential decrease law to background level follow. Fig. 6 depicts the PSC recording of the fourth abrupt uniaxial compressional stress step, on a logarithmic current axis with respect to time. It is evident that after the appearance of the  $PSC_{\text{peak}}$ , two relaxation processes occur. Fitting PSC values as a function of time indicates that an exponential relaxation law should exist, with an initially short relaxation time  $\tau_1$  followed by a fairly longer  $\tau_2$ . Such a relaxation can be empirically described by the relation in Eq. (6).

$$I(t) = A_1 \cdot \exp\left(-\frac{t}{\tau_1}\right) + A_2 \cdot \exp\left(-\frac{t}{\tau_2}\right) \quad (6)$$

where  $A_1$  and  $A_2$  are constants. Results from other experiments conducted on materials like marble and amphibolite, are verified qualitatively [15] and [20]. After the PSC becomes maximum and taking into account that the stress remains constant, the microcrack production rate decreases rapidly and consequently the PSC decreases with a short relaxation time  $\tau_1$ . This decrease does not continue at the same rate because another mechanism may keep the PSC for a long time, so

that the PSC relaxation takes place with a longer time constant  $\tau_2$ .

A probable cause is the continuing material strain, even at a very low rate, although stress is unchanged. The new microcracks that go on appearing produce new microcurrents and result in conserving PSC at relatively high values that do not permit a direct relaxation to noise level.

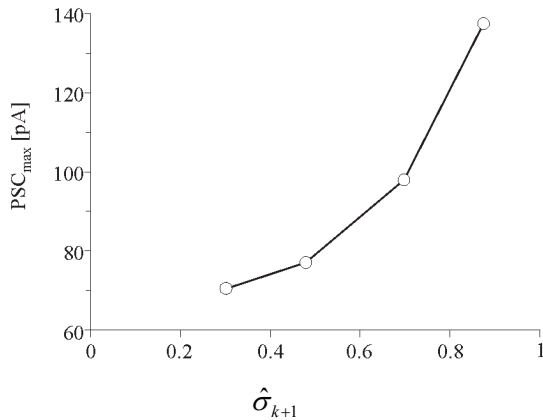


Fig. 7. Correlation of the  $PSC_{peak}$  values with respect to the final stress level  $\hat{\sigma}_{k+1}$

The  $PSC_{peak}$  value of each PSC following the application of an abrupt stepwise uniaxial compressional stress depends on the final state  $\sigma_k + 1$ .

In Table 2,  $PSC_{peak}$  values can be read with respect to the initial  $\sigma_k$  and the final  $\sigma_k + 1$  states of each stress step, as well as with the respective relative compressional stress states  $\hat{\sigma}_k$  and  $\hat{\sigma}_{k+1}$ . Fig. 7 depicts graphically the  $PSC_{peak}$  values with respect to the corresponding values of the final state  $\hat{\sigma}_{k+1}$  of each step. The final states  $\hat{\sigma}_{k+1}$  of steps 3 and 4 correspond to stress values which have driven the material into the non-linear deformation range ( $\hat{\sigma}_{k+1} > 0.7$ ). The  $PSC_{peak}$  values are evidently greater than the initial. A similar behaviour has been observed in laboratory experiments using the SST technique on marble samples [12].

Table 2 shows the calculated values of the totally emitted electric charge  $Q$  during the four sequential abrupt stress increases as well as the values of the relaxation time constants  $\tau_1$  and  $\tau_2$ .

An intense increase of the electric charge can be observed (Fig. 8), as long as the value of the final state  $\hat{\sigma}_{k+1}$  in which the material will relax

after the abrupt stepwise uniaxial compressional stress procedure. Such an increase is directly related with the continuously increasing  $PSC_{peak}$  value (Fig. 7), and with the values of the relaxation time constants  $\tau_1$  and  $\tau_2$ , which, as it becomes evident from Table 2, keep on increasing with the value of the final state  $\hat{\sigma}_{k+1}$ .

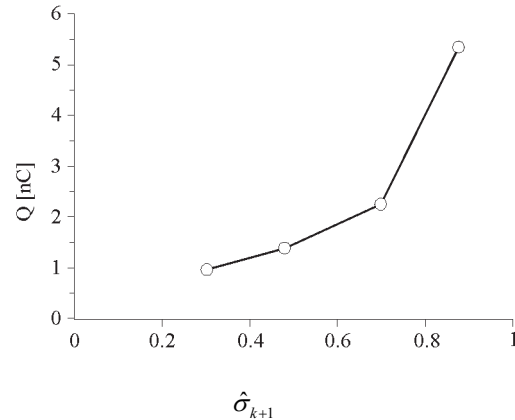


Fig. 8. Correlation of the totally emitted electric charge with respect to final stress level  $\hat{\sigma}_{k+1}$

#### 4 CONCLUSIONS

PSC laboratory experiments were conducted on hardened cement mortar samples. It was found that the used samples exhibit a familiar behaviour, which has similarities to those of rocks like marble and amphibolite. In the present work, the experimental results can be summarised as follows:

From the microphysical point of view it is noted that in the non-linear deformation range micro structural changes occur within the samples depending on the stress magnitude. They constitute the dominant form of all heterogeneities that determine the process of eventual failure. In particular, in the cement mortar there is a transition zone between the aggregate and the hydrated cement paste which constitutes a region of relative weakness containing a number of microcracks even before loading, during the shrinkage state. The increasing number of microcracks at the lateral edges of shear cracks reaches a minimum critical distance with respect to each other and begins to merge.

Table 2. Values of the parameters of the SST technique ( $b \approx 5$  MPa/s)

step	$\sigma_k$ [MPa]	$\sigma_{k+1}$ [MPa]	$\hat{\sigma}_k$	$\hat{\sigma}_{k+1}$	$PSC_{peak}$ [pA]	$\tau_1$ [s]	$\tau_2$ [s]	$Q$ [nC]
1	5.5	14.5	0.11	0.30	70.5	5.6	159	0.95
2	14.5	23.0	0.30	0.48	77.1	7.4	182	1.38
3	23.0	33.5	0.48	0.70	98.0	9.1	227	2.25
4	33.5	42.0	0.70	0.88	137.5	13.1	294	5.34

The above are directly correlated with the emission of weak electric currents in all of the used techniques of mechanical stress. Both qualitative and quantitative characteristics of the Pressure Stimulated Currents may show the stress range to which the sample has been subjected.

Summarizing, PSC measurements can provide a prediction of the stress state of the material relative to the crack openings and in general to the stages of composite damage.

#### 5 ACKNOWLEDGEMENTS

The authors wish to thank Prof. Z. Agioutantis, Director of the Rock Mechanics Laboratory of the Technical University of Crete for providing the equipment to draw the stress-strain diagram of the cement mortar samples.

#### 6 REFERENCES

- [1] Nitsan, U. (1977). Electromagnetic emission accompanying fracture of quartz-bearing rocks. *Geophysical Research Letters*, vol. 4, p. 333-337.
- [2] Ogawa, T., Oike, K., Mirura, T. (1985). Electromagnetic radiations from rocks. *J. Geophys. Res.*, vol. 90, p. 6245-6249.
- [3] Ishido, T., Mizutani, H. (1981). Experimental and theoretical basis of electrokinetic phenomena in rock-water systems and its applications to geophysics. *J. Geophys. Res.*, vol. 86, p. 1763-1775.
- [4] Yoshida, S., Clint, O.C., Sammonds, P.R. (1998). Electric potential changes prior to shear fracture in dry and saturated rocks. *Geophys. Res. Letters*, vol. 25, p. 1577-1580.
- [5] Varotsos, P., Alexopoulos, K. (1986). *Thermodynamics of point defects and their relation with bulk properties*. North-Holland, Amsterdam.
- [6] Hadjicontis, V., Mavromatou, C. (1994). Transient electric signals prior to rock failure under uniaxial compression. *Geophys. Res. Letters*, vol. 21, p. 1687-1990.
- [7] Brady, B.T., Rowell, G.A. (1986). Laboratory investigation of the electrodynamics of rock fracture. *Nature*, vol. 321, p. 448-492.
- [8] Enomoto, J., Hashimoto, H. (1990). Emission of charged particles from indentation fracture of rocks. *Nature*, vol. 346, p. 641-643.
- [9] Vallianatos, F., Tzanis, A. (1998). Electric current generation associated with the deformation rate of a solid: Preseismic and coseismic signals. *Physics and Chemistry of the Earth*, vol. 23, p. 933-938.
- [10] Vallianatos, F., Tzanis, A. (1999). A model for the generation of precursory electric and magnetic fields associated with the deformation rate of the earthquake focus. Hayakawa, M. (ed.), *Atmospheric and Ionospheric electromagnetic phenomena associated with Earthquakes*, Terra Scientific Publishing Co, Tokyo.
- [11] Vallianatos, F., Triantis, D., Tzanis, A., Anastasiadis, C., Stavrakas, I. (2004). Electric earthquake precursors: from laboratory results to field observations. *Physics and Chemistry of the Earth*, vol. 29, p. 339-351.
- [12] Anastasiadis, C., Triantis, D., Stavrakas, I., Vallianatos, F. (2004). Pressure stimulated currents (PSC) in marble samples after the application of various stress modes before fracture. *Annals of Geophysics*, vol. 47, p. 21-28.
- [13] Anastasiadis, C., Triantis, D., Hogarth, C.A. (2007). Comments on the phenomena

- underlying pressure stimulated currents (PSC) in dielectric rock materials. *Journal of Materials Science*, vol. 42, p. 2538-2542.
- [14] Triantis, D., Stavrakas, I., Anastasiadis, C., Kyriazopoulos, A., Vallianatos, F. (2006). An analysis of Pressure Stimulated Currents (PSC), in marble samples under mechanical stress. *Physics and Chemistry of the Earth*, vol. 31, p. 234-239.
- [15] Triantis, D., Anastasiadis, C., Vallianatos, F., Kyriazis, P., Nover, G. (2007). Electric signal emissions during repeated abrupt uniaxial compressional stress steps in amphibolite from KTB drilling. *Natural Hazards and Earth System Sciences*, vol. 7, p. 149-154.
- [16] Stavrakas, I., Triantis, D., Agioutantis, Z., Maurigiannakis, S., Saltas, V., Vallianatos, F., Clarke, M. (2004). Pressure stimulated currents in rocks and their correlation with mechanical properties. *Natural Hazards and Earth System Sciences*, vol. 4, p. 563-567.
- [17] Sun, M., Liu Li, Q.Z., Wang, E. (2002). Electrical emission under low compressive loading. *Cement and Concrete Research*, vol. 32, p. 47-50.
- [18] Sun, M., Li, Z., Song, X. (2004). Piezoelectric effect of hardened cement paste. *Cement and Concrete Composites*, vol. 26, p. 717-720.
- [19] Tzani, A., Vallianatos, F. (2002). A physical model of electrical earthquake precursors due to crack propagation and the motion of charged edge dislocations. Hayakawa, M., Molchanov, O.A. (eds.), *Seismo Electromagnetics: Lithosphere-Atmosphere-Ionosphere Coupling*, TERRAPUB, Tokyo, p. 117-130.
- [20] Tzani, A., Vallianatos, F., Gruszow, S. (2000). Identification and discrimination of transient electrical earthquake precursors: Fact, fiction and some possibilities. *Phys. Earth Planet Int.*, vol. 121, p. 223-248.
- [21] Whitworth, R.W. (1975). Charged dislocations in ionic crystals. *Advances in Physics*, vol. 24, p. 203-304.
- [22] Pomeroy, C.D. (1980). Physics in cement and concrete technology. *Physics Education*, vol. 15, p. 171-176.
- [23] Kyriazis, P., Anastasiadis, C., Triantis, D., Vallianatos, F. (2006). Wavelet analysis on Pressure Stimulated Currents emitted by marble samples. *Natural Hazards and Earth System Sciences*, vol. 6, p. 889-894.